# Removal of NO in NO/N$_2$, NO/N$_2$/O$_2$, NO/CH$_4$/N$_2$, and NO/CH$_4$/O$_2$/N$_2$ Systems by Flowing Microwave Discharges

**José L. Hueso,[†] Agustín R. González-Elipe,[†] José Cotrino,\*,[†,‡] and Alfonso Caballero[†,§]**

*Instituto de Ciencia de Materiales de Sevilla (CSIC-Universidad de Sevilla), Avda Américo Vespucio 49, 41092 Sevilla, Spain, and Departamento de Química Inorgánica, Facultad de Química, and Departamento de Física Atómica, Molecular y Nuclear, Universidad de Sevilla, 41092 Sevilla, Spain*

In this paper, continuing previous work, we report on experiments carried out to investigate the removal of NO from simulated flue gas in nonthermal plasmas. The plasma-induced decomposition of small concentrations of NO in N$_2$ used as the carrier gas and O$_2$ and CH$_4$ as minority components has been studied in a surface wave discharge induced with a surfatron launcher. The reaction products and efficiency have been monitored by mass spectrometry as a function of the composition of the mixture. NO is effectively decomposed into N$_2$ and O$_2$ even in the presence of O$_2$, provided always that enough CH$_4$ is also present in the mixture. Other majority products of the plasma reactions under these conditions are NH$_3$, CO, and H$_2$. In the absence of O$_2$, decomposition of NO also occurs, although in that case HCN accompanies the other reaction products as a majority component. The plasma for the different reaction mixtures has been characterized by optical emission spectroscopy. Intermediate excited species of NO$^*$, C$^*$, CN$^*$, NH$^*$, and CH$^*$ have been monitored depending on the gas mixture. The type of species detected and their evolution with the gas composition are in agreement with the reaction products detected in each case. The observations by mass spectrometry and optical emission spectroscopy are in agreement with the kinetic reaction models available in literature for simple plasma reactions in simple reaction mixtures.

## I. Introduction

During the last years, nonthermal plasma procedures have been presented as a competitive technology for air cleaning and now it is clear that the reduction of pollutants from industrial processes and vehicle exhausts is one of the critical and urgent topics in environmental and pollution control research. Removal of NO from gas streams is one of the most challenging problems in this context. Its removal has been intended by means of different plasma procedures including barrier discharge plasmas (DBD),[1−5] corona discharges,[2,5−9] microwave plasmas (MW),[10−12] ac plasmas,[13] and hollow cathode plasmas.[14] As a general rule, in DBD discharges the presence of oxygen tends to produce the oxidation of NO to NO$_2$,[5,6] while in MW discharges dissociation of NO into N$_2$ and O$_2$ usually occurs.[15,16]

Many works in the literature dealing with this subject aim at describing the decomposition and/or reaction mechanisms of simple mixtures of NO with inert carrier gases or air.[2,4,5,13,17,18] Fewer works have addressed the fundamental problems involved during the removal of NO from complex mixtures as those existing in real combustion exhausts.[19,20] For example, gases produced by diesel engines and other combustion processes are a complex mixture of N$_2$ (majority component), remaining oxygen, CO$_2$, unburned hydrocarbons, water vapor, and soot particles in suspension.[21,22] The plasma chemistry of such complex mixtures is not easy, and its description and eventual

optimization for NO removal requires a thorough assessment of the influence of the different plasma parameters (e.g., electric field frequency, microwave power, gas pressure, gas flow, reactor geometry, etc.) and a specific evaluation of the influence of the elemental reaction processes involved.

Flowing discharges containing nitrogen oxide have been the subject of different studies during the last years. Thus, the study of the kinetics of NO$_x$ (i.e., NO + NO$_2$) in spatially homogeneous dc low-pressure discharges has been performed both theoretically and experimentally by Gordiets et al.[23] Similar reactions and the related kinetic models for flowing microwave discharges and postdischarges in N$_2$/O$_2$ mixtures have also raised much interest in the context of plasma sterilization processes and other industrial applications.[24−26] From these studies, for pressures above approximately 1 Torr and for values of reduced electric field strength (i.e., E/N $\sim$ 8 $\times$ 10$^{-16}$ V cm$^2$), a relatively high dissociation yield of NO should be expected in nitrogen glow discharges.[27] On the other hand, the decomposition of methane in nitrogen discharges has been the subject of numerous studies of interest in fields such as detoxification, atmospheric chemistry, synthesis, metal nitriding, etc.[28−30] From these and other studies, the kinetics of the methane decomposition in nitrogen plasmas has been established and the main dissociation mechanisms of CH$_4$ in a N$_2$/CH$_4$ mixtures have been proposed.[29−31] However, similar fundamental studies with more complex plasma mixtures are still scarce.[32] In this context, in a previous work using a surface wave (SW) setup and Ar as the carrier gas we have studied the MW plasma chemistry of complex mixtures of NO with other minority components such as hydrocarbons, oxygen, or nitrogen.[15] A 90% amount of NO removal can be achieved with mixtures of Ar/NO/O$_2$/CH$_4$. The addition of low amounts of N$_2$ and O$_2$ produced a decrease in

* To whom correspondence should be addressed. Fax: +34 954460665. E-mail: cotrino@us.es.
† Instituto de Ciencia de Materiales de Sevilla (Centro Mixto CSIC-Universidad de Sevilla).
‡ Departamento de Física Atómica, Molecular y Nuclear, Universidad de Sevilla.
§ Departamento de Química Inorgánica, Universidad de Sevilla.

**TABLE 1: Reaction Products for $N_2 + O_2 + NO$ Mixtures Containing Different Concentrations of $O_2$**

| reacn mixture | NO decomposn (%) | reacn products |
|---|---|---|
| $N_2 + NO$ | 97 | $N_2$, $O_2$, $N_2O$ (traces) |
| $N_2 + NO + O_2$ (1%) | 95 | $N_2$, $O_2$, $N_2O$ (traces) |
| $N_2 + NO + O_2$ (3%) | 70 | $N_2$, $O_2$, NO, $N_2O$ (traces) |
| $N_2 + NO + O_2$ (5%) | 40 | $N_2$, NO, $N_2O$ (traces) |

the decomposition yield, a feature that suggests that even smaller yields of decomposition might be obtained if $N_2$ is used as carrier gas. To address this question, in this work we have studied similar reactions by substituting Ar by $N_2$ as carrier gas. This experimental situation is closer to that existing in real exhausts, and therefore, the extrapolation of the obtained results to real working conditions could be more straightforward. As in the previous work using Ar as the carrier gas, here we have analyzed the different reaction products by mass spectrometry (MS) and identified intermediate species in the plasma by optical emission spectroscopy (OES). The obtained results have evidenced that the decomposition of NO into $N_2$ and $O_2$ is very high even in the presence of oxygen, provided that $CH_4$ is added to the reaction mixture. Plasma reactors require a very complex modeling because of the self-consistent coupling of the fluid dynamics, electrodynamics phenomena, and reaction kinetics. In this work, we have mainly focused on the chemical mechanisms trying to account for the removal of NO as a result of chemical reactions in the nonthermal plasma phase. For this purpose, we have considered the kinetic data available in the literature for simple reactions, involving radicals and excited species. Thus, these reactions provide a comprehensive description of more complex reaction processes taking place under our experimental conditions.

## II. Experimental Section

A scheme of the experimental setup is reported in a previous work.[15] The plasma reactor consists of a quartz tube of 3.5 mm inner diameter. The plasma is produced by a 2.45 GHz surfatron exciter. Microwave power is transported from the power supply to the surfatron via a coaxial cable coupled with a slot antenna directly connected to the launcher. A power of 60 W was used in the experiments. Although this parameter was not modified for the series of experiments reported here, it is worth noting that very similar results were also obtained for smaller powers down to 20 mW, a value at which the plasma already extinguished. The traveling microwave power and the electron density decrease from the excitation gap to the plasma end, where the electron density reaches its critical value (approximately $3.7 \times 10^{11}$ cm$^{-3}$ at 2450 MHz). The gas mixtures were prepared with mass flow controllers connected to the entrance of the quartz tube. The mass flow of $N_2$ used as carrier gas was fixed at 25 sccm. Typical compositions of gas mixtures were as follows: NO (3000 ppm); $O_2$ (from 0 to 5% in volume); $CH_4$ (from 0 to 5000 ppm). The total pressure in the reactor was controlled by adjusting a throttle valve placed between the reactor and a vacuum pump. Experiments were carried out for different compositions of the gas mixtures around the aforementioned values and a total pressure of 45 torrs. This parameter was maintained fixed in all the experiments since no significant changes in reaction efficiency were observed between 30 and 75 torrs. Plasma extends over a few centimetres and is followed by a homogeneous afterglow along the postdischarge. Analysis of the gas mixtures before and after plasma ignition was done by mass spectrometry (MS) (QMS 422 from Balzers). The gases were sampled to the mass spectrometer through a calibrated
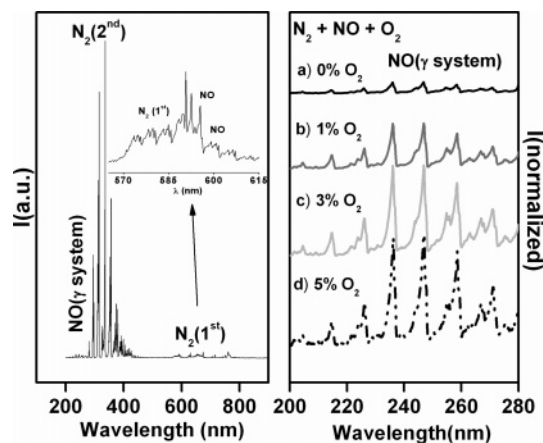


**Figure 1.** Left: Wide scan OES spectrum of a $N_2 + O_2 + NO$ mixture. The inset shows in an enlarged scale the bands due to the first positive $N_2$ system and the NO bands first reported by Tanaka et al.[33] Right: Series of spectra for the zone comprised between 200 and 280 nm corresponding to the vibrational bands of NO* species for different concentrations of $O_2$. The intensity of the bands has been normalized to the intensity of the $N_2$* peak at 337.13 nm.

leak valve. When possible, calibration of the peak intensities is carried out with simple mixtures of $N_2$ with either the reactants or the gases obtained as products of the reactions. The accuracy of the analysis is considered to be within 12% of maximum uncertainty. The induction period to reach steady-state conditions was very small, in any case shorter than 10 s.

Study of the plasma by OES is carried out by collecting the light with an optical fiber and analyzing the emitted spectra with a Jobin Ybon (HR250) scanning monochromator and a Hamamatsu photomultiplier tube (R928). The whole system was operated and the signals were collected with a personal computer.

## III. Results

**A. Mixtures $N_2$/NO and $N_2$/NO/$O_2$.** The plasma activation in the SW reactor of a $N_2$/NO mixture yields $O_2$ as majority detectable product with a NO decomposition efficiency of 97% as reported in Table 1. An equivalent amount of $N_2$ is supposed to be formed, although its determination by MS was not possible because this product is also the carrier gas. This result indicates that even in the presence of a high concentration of $N_2$, the NO is effectively dissociated by a flowing SW plasma excitation. By MS analysis it is also possible to detect the formation of traces of $N_2O$ as a minority product. As reported in Table 1, the addition of $O_2$ to the reaction mixture produces a decrease in the efficiency of the process that reaches only a 40% NO dissociation for a concentration of 5% oxygen and of 70% for 3% oxygen. This dissociation yield is higher than the 42% found previously in a SW discharge for Ar + $N_2$ (3%) + $O_2$ (3%) + NO mixtures.[15]

Interesting hints about the reaction mechanism can be obtained by the OES detection of the intermediate species of the plasma. Figure 1 (left) shows a wide scan spectrum comprising the main bands found for the $N_2$/$O_2$/NO system. The bands of the second positive system of $N_2$ (bands from 280 to 497 nm, $N_2(C^3\Pi_u, v' = 4 \rightarrow N_2(B^3\Pi_g, v'' = 4) + h\nu$, at 326.8 nm)[33] are relatively more intense than the others. Therefore, these bands are used for the normalization of the OES spectra. The bands of the nitrogen first positive system ($N_2(B^3\Pi_g, v' = 6 \rightarrow N_2(A^3\Sigma_u^+, v'' = 1) + h\nu$, at 662.3 nm) present a smaller intensity and are also depicted in an enlarged scale in that figure. The NO$\gamma$ system, produced by radiative decay of NO($A^2\Sigma^+$)

**TABLE 2: Summary and Attribution of the Main Bands Detected by OES for the Different Gas Mixtures**

| reacn mixture | species (system) | electronic transitions | peaks and bands intervals |
|---|---|---|---|
| $N_2 + NO + O_2$ | $N_2$ (2nd positive system) | $C\,^3\Pi \rightarrow B\,^3\Pi$ | 281.43−497.64 |
| | $N_2$ (1st positive system) | $B\,^3\Pi \rightarrow A^3\Sigma$ | 503.08−10420 |
| | NO ($\gamma$ system) | $A^2\Sigma^+ \rightarrow {}^2\Pi$ | 195.61−345.85 |
| | $N_2^+$ (main system) | ${}^2\Sigma \rightarrow {}^2\Sigma$ | 329.34−586.47 |
| | NO (Tanaka et al.) | | 523.22−642.94 |
| $N_2 + NO + CH_4$ | $N_2$ (2nd positive system) | $C\,^3\Pi \rightarrow B\,^3\Pi$ | 281.43−497.64 |
| | $N_2$ (1st positive system) | $B\,^3\Pi \rightarrow A\,^3\Sigma$ | 503.08−10420 |
| | NO ($\gamma$ system) | $A\,^2\Sigma^+ \rightarrow {}^2\Pi$ | 195.61−345.85 |
| | $N_2^+$ (main system) | ${}^2\Sigma \rightarrow {}^2\Sigma$ | 329.34−586.47 |
| | NO (Tanaka et al.) | | 523.22−642.94 |
| | NH (3360 A system) | ${}^3\Pi \rightarrow {}^3\Sigma$ | 336.00−337.00 |
| | CN (violet system) | ${}^2\Sigma \rightarrow {}^2\Sigma$ | 358.59−460.61 |
| | CN (red system) | ${}^3\Pi \rightarrow {}^2\Sigma$ | 437.38−939.30 |
| | CH (A 4300 system) | ${}^2\Delta \rightarrow {}^2\Pi$ | 431.25−494.00 |
| | N I | ${}^4P° \rightarrow {}^4P$ | 672.09 |
| | C I | ${}^1S \rightarrow {}^1P°$ | 247.86 |
| | H | ${}^1P° \rightarrow {}^2D$ | 656.28 |
| $N_2 + CH_4 + O_2$ | $N_2$ (2nd positive system) | $C\,^3\Pi \rightarrow B\,^3\Pi$ | 281.43−497.64 |
| | $N_2$ (1st positive system) | $B\,^3\Pi \rightarrow A\,^3\Sigma$ | 503.08−10420 |
| | NO ($\gamma$ system) | $A\,^2\Sigma^+ \rightarrow {}^2\Pi$ | 195.61−345.85 |
| | $N_2^+$ (main system) | ${}^2\Sigma \rightarrow {}^2\Sigma$ | 329.34−586.47 |
| | NH (3360 A system) | ${}^3\Pi \rightarrow {}^3\Sigma$ | 336.00−337.00 |
| | CN (violet system) | ${}^2\Sigma \rightarrow {}^2\Sigma$ | 358.59−460.61 |
| | CN (red system) | ${}^3\Pi \rightarrow {}^2\Sigma$ | 437.38−939.30 |
| | CH (A 4300 system) | ${}^2\Delta \rightarrow {}^2\Pi$ | 431.25−494.00 |
| | N I | ${}^4P° \rightarrow {}^4P$ | 672.09 |
| | C I | ${}^1S \rightarrow {}^1P°$ | 247.86 |
| | H | ${}^1P° \rightarrow {}^2D$ | 656.28; 486.13 |
| $N_2 + CH_4 + O_2 + NO$ | $N_2$ (2nd positive system) | $C\,^3\Pi \rightarrow B\,^3\Pi$ | 281.43−497.64 |
| | $N_2$ (1st positive system) | $B\,^3\Pi \rightarrow A\,^3\Sigma$ | 503.08−10420 |
| | $N_2^+$ (main system) | ${}^2\Sigma \rightarrow {}^2\Sigma$ | 329.34−586.47 |
| | NO ($\gamma$ system) | $A\,^2\Sigma^+ \rightarrow {}^2\Pi$ | 195.61−345.85 |
| | NH (3360 A system) | ${}^3\Pi \rightarrow {}^3\Sigma$ | 336.00−337.00 |
| | CN (violet system) | ${}^2\Sigma \rightarrow {}^2\Sigma$ | 358.59−460.61 |
| | N I | ${}^4P° \rightarrow {}^4P$ | 672.09 |
| | H | ${}^1P° \rightarrow {}^2D$ | 656.28 |

**TABLE 3: Reaction Products for $N_2 + CH_4 + O_2$ Mixtures Containing Different Concentrations of $O_2$**

| reacn mixture | $O_2$ conversn (%) | $CH_4$ removal (%) | reacn products (ppm) |
|---|---|---|---|
| $N_2 + CH_4$ | | 100 | $H_2$, HCN (<3000), $NH_3$ (<3000), $H_2O^a$ (traces) |
| $N_2 + CH_4 + O_2$ (0.3%) | 98 | 100 | $H_2$, $NH_3$ (<500), $H_2O$ (<4500), CO (<1600), HCN (<1400) |
| $N_2 + CH_4 + O_2$ (1%) | 65 | 100 | $H_2$, $NH_3$, $H_2O$ (<8400), CO (<2900), $N_2O$ (<300) |
| $N_2 + CH_4 + O_2$ (3%) | 28 | 100 | $H_2$, $NH_3$, CO (<2000), $H_2O$ (<8000), $CO_2$ (<400), $N_2O$ (traces), NO (traces) |

$^a$ $H_2O$ from humidity on the walls of the reactor

excited states, is detected at 247.9 nm. By contrast, NO$\beta$ emission bands are not observed in our system.[33] It is also interesting the appearance of some peculiar bands in the range 523−643 nm which have been assigned to NO* (i.e., excited NO) by other authors (Tanaka et al. and Grillet et al.).[33] Figure 1 (right) shows different spectra of the NO $\gamma$ system corresponding to the vibrational structure of NO* species detected in the range 200−280 nm for $N_2 + NO$ and $N_2 + O_2 + NO$ mixtures with different concentrations of $O_2$. This figure shows that the intensity of the NO* bands increases as the amount of $O_2$ in the mixture increases. A summary of the assignments of the different bands and peaks detected under the different conditions explored in this work is presented in Table 2.

**B. $N_2/CH_4$ and $N_2/CH_4/O_2$ Mixtures.** Real exhaust mixtures coming from diesel and other combustion processes contain, among other components, unburned hydrocarbons. Therefore, it is pertinent to study the plasma reactions of hydrocarbons and oxygen as minority components and $N_2$ as carrier gas as a preliminary step prior to the consideration of complex mixtures containing NO. Table 3 summarizes the main products of the plasma reactions detected by MS analysis for mixtures with three different concentrations of oxygen.

In all cases, $CH_4$ reacts almost completely (i.e., decomposition yield higher than 99%). This indicates that oxygen is used to burn the methane. For the $N_2/CH_4$ mixture without oxygen, the products of the reaction are HCN, $H_2$, and $NH_3$ plus some traces of $H_2O$ from the inner walls of the reactor. Meanwhile, for $N_2/O_2/CH_4$ mixtures, besides $NH_3$ and traces of HCN, reactions products such as $H_2O$ and CO are formed for $O_2$ concentrations between 0.3% and 1%. For an oxygen concentration of 3%, CO and $H_2O$ are major products with $CO_2$ and $N_2O$ appearing in the range of traces. This change in reaction products for relatively high concentration of $O_2$ can be accounted by assuming that the total oxidation of methane (i.e., a process based on the overall equation $CH_4 + 3/2O_2 \rightarrow CO + 2H_2O$, whereby a minimum of 1.5 molecules of $O_2$ are required for each of $CH_4$) is favored with respect to the other reactions involving nitrogen. The most significant difference in comparison with previously reported results with Ar is that neither solid carbon deposits nor higher hydrocarbon species (i.e. $C_2H_y$) are produced in poor oxygen mixtures. Instead, HCN, $NH_3$, and $H_2O$ are the main products obtained with $N_2$ as carrier gas (see Table 3). However, when relatively high concentrations of $O_2$ are present, the reaction products are similar for both carrier
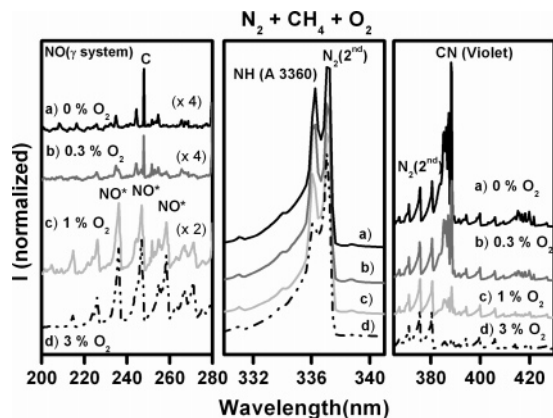
**Figure 2.** OES spectra for $N_2 + CH_4 + O_2$ mixtures for different concentrations of oxygen at fixed $CH_4$ values (3000 ppm): (a) $N_2 + CH_4 + O_2$ (0%); (b) $N_2 + CH_4 + O_2$ (0.3%); (c) $N_2 + CH_4 + O_2$ (1%); (d) $N_2 + CH_4 + O_2$ (3%). Left: Bands attributed to $NO^*$ and $C^*$ species. Middle: Bands attributed to $N_2^*$ and $NH^*$ species. Right: Bands attributed to $N_2^*$ and $CN^*$ species.
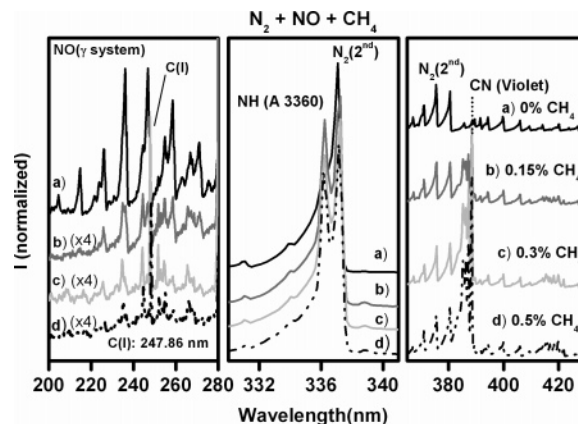


**Figure 3.** OES spectra for mixtures $N_2 + NO + CH_4$ for different concentrations of $CH_4$: (a) $N_2/NO/CH_4$ (0%); (b) $N_2/NO/CH_4$ (0.15%); (c) $N_2/NO/CH_4$ (0.3%); (d) $N_2/NO/CH_4$ (0.5%). Left: Bands attributed to $NO^*$ and $C^*$ species. Middle: Bands attributed to $N_2^*$ and $NH^*$ species. Right: Bands attributed to $N_2^*$ and $CN^*$ species.

gases. These products basically result from the partial oxidation of $CH_4$, HCN, and $NH_3$.

The OES analysis of the plasma shows the formation of various intermediate species. The spectra collected for different relative concentrations of $O_2$ are reported in Figure 2. At first sight, the bands due to $NO^*$ increase in intensity, while those due to $CN^*$ diminish as the amount of $O_2$ in the reaction mixture increases. In comparison with the OES spectra recorded for mixtures $Ar/CH_4/O_2$, an important difference is that bands due to $C_2^*$ species, detected when using Ar as the carrier gas, are not detected in the present case. This fact suggests that $C_2^*$ are intermediate species in the formation of the solid carbon, a majority product obtained with mixtures $Ar/CH_4$. For mixtures $N_2/CH_4/O_2$ atomic $C^*$ species (see Figure 2 (left)), characterized by a narrow peak at 247.86 nm (see Table 2), $NH^*$ species (peak at 336.0 nm), and $CH^*$ bands in the range of 425−445 nm are the most significant species observed in the spectra of Figure 2. The $CN^*$ species, giving rise to a series of bands at around 388 nm when no oxygen is present in the mixture (red system; see Table 2), proves the relevant role of $CN^*$ intermediate reaction species in the plasma reactions under these lean-$O_2$ conditions.

The formation of $NH_3$ as reaction product is indicated by the identification of $NH^*$ intermediate species in the OES spectra (see Figure 2). It is worth noting that the intensity of the corresponding band decreases as the amount of $O_2$ is enhanced. This fact suggests that active species of nitrogen associate with oxygen instead of H, when $O_2$ is present in the reaction mixture. In this sense, we observed the existence of atomic lines for $N^*$ (672.09 nm) and $H^*$ (656.28 nm) (see Table 2) which might be directly related to the dissociation of this NH intermediate, since they only appear when $CH_4$ is introduced in the mixture and there is no relevant emission signal of them in the ternary $N_2/NO/O_2$ mixtures from the previous section. A similar behavior can be observed with regard to $C^*$ and $CH^*$ intermediates, whose intensities decrease as the concentration of oxygen increases (data not shown).

**C. Mixtures $N_2/NO/CH_4$.** Essays with this mixture were carried out for three different concentrations of $CH_4$, namely 0.15, 0.30, and 0.50%. These low concentrations of $CH_4$ have been selected on purpose to check whether the dissociation pattern of $CH_4$ may be affected by NO. Note in this respect that the reductive power of one molecule of $CH_4$ is equivalent, at least, to three molecules of NO (i.e., $CH_4 + 3NO \rightarrow 3/2N_2 + 2H_2O + CO$). The results summarized in Table 4 indicates that both reactants, NO and $CH_4$, are almost completely decomposed by the plasma and that the majority products of this reaction are CO, HCN, and $H_2O$ ($H_2$). In comparison with the results reported for mixtures $Ar/CH_4/NO$, the main difference resides on the lack of detection of $C_2$ or higher hydrocarbons.

The OES analysis of the plasma reported in Figure 3 reveals the formation of excited species of $N_2^*$ (second positive system), $CN^*$ (violet and red system), and $NH^*$ (A 3360). $CH^*$ (A 4300 system), $N^*$ (672.09 nm), and $H^*$ ($H_\alpha$, $H_\beta$) intermediates are also detected but not appreciably in the figure (see Table 2). In addition, the narrow peak at 247.86 nm, attributed to $C^*$ atomic species (see Table 2), is also recorded. It has a maximum intensity for a concentration of 0.5% $CH_4$. It is also noteworthy in this figure that the intensity of the NO$\gamma$ bands decreases while the $CN^*$ bands increase with the concentration of $CH_4$ in the mixture. Meanwhile, the intensity of the band due to $NH^*$ species remains practically constant, once $CH_4$ is added, regardless the concentration in the mixture (see Figure 3 (right)).

The reductive effect of $CH_4$ in the plasma reaction is evidenced in Figure 3 (left) by the decrease of intensity of the $NO^*$ bands as the percentage of methane in the mixture increases. Meanwhile, the formation of HCN is congruent with the monitoring by OES of high-intensity bands due to $CN^*$ intermediates (violet system displayed in Figure 3 (right) and red system not displayed).

**D. Mixtures $N_2/NO/O_2/CH_4$.** This mixture represents the best approach under our experimental conditions to the composition of real exhausts (note, however, that real exhausts are much more complex with the presence of water vapor, $CO_2$, soot particles, and eventually higher hydrocarbons). A series of tests

**TABLE 4: Reaction Products for $N_2 + NO + CH_4$ Mixtures Containing Different Concentrations of $CH_4$**

| reacn mixture | NO removal (%) | $CH_4$ removal (%) | reacn products (ppm) |
|---|---|---|---|
| $N_2 + NO$ | 97 | | $N_2$, $O_2$, $N_2O$ (traces) |
| $N_2 + NO + CH_4$ (0.15%) | 100 | 100 | $H_2$, HCN (<700), CO (<800), $NH_3$ (<1400), $H_2O$ (<2200) |
| $N_2 + NO + CH_4$ (0.30%) | 100 | 98 | $H_2$, HCN (<1300), CO (<1700), $NH_3$ (<1400), $H_2O$ (<1300) |
| $N_2 + NO + CH_4$ (0.50%) | 100 | 96 | $H_2$, HCN (<3400), CO (<1600), $NH_3$ (<1300), $H_2O$ (<1400) |

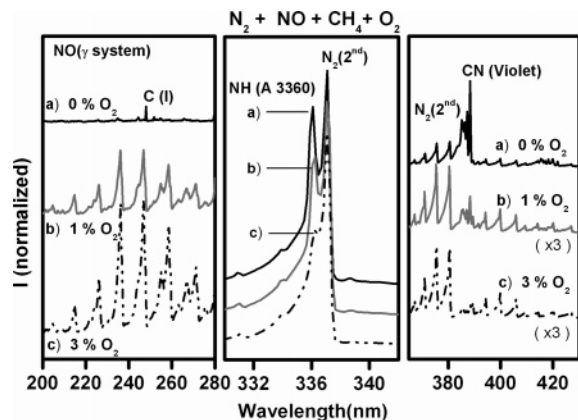**Figure 4.** OES spectra for $N_2 + NO + CH_4 + O_2$ mixtures for different concentrations of oxygen at fixed $CH_4$ values (3000 ppm): (a) $N_2 + NO + CH_4 + O_2$ (0%); (b) $N_2 + NO + CH_4 + O_2$ (1%); (c) $N_2 + NO + CH_4 + O_2$ (3%). Left: Bands attributed to $NO^*$ and $C^*$ species. Middle: Bands attributed to $N_2^*$ and $NH^*$ species. Right: Bands attributed to $N_2^*$ and $CN^*$ species.

have been done by varying the concentration of $CH_4$ and $O_2$ in the mixture. A summary of the reaction products detected in each case, as well as efficiency data with respect to the decomposition of NO, is reported in Table 5. In all cases, the majority reaction products were CO and $H_2O$, while $CO_2$ and $N_2O$ were detected as traces. On the other hand, while $CH_4$ decomposes almost completely in all cases, the percentage of decomposition of NO decreases as the amount of oxygen in the mixture increases.
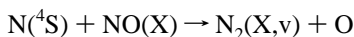
The NO removal efficiency reaches only about 60% for an oxygen concentration of 3%. It is interesting that 100% decomposition is found when the concentration of $O_2$ is a minimum (i.e., 1%) and that of $CH_4$ a maximum (i.e., 0.5%)

Figure 4 shows the OES spectra detected for these quaternary mixtures. The detected peaks and bands correspond to $N_2^*$, $NO^*$, $NH^*$, and $CN^*$ excited-state species (Table 2). The addition of higher concentrations of oxygen to the mixture leads to an increase in the number of $NO^*$ species (Figure 4 (left)) and a decrease of that of $CN^*$, $H^*$, $N^*$, $C^*$, and $NH^*$ intermediates (Figure 4). For greater concentrations of $CH_4$ (i.e., 0.5%) the same type of bands are detected, although the intensity for the species involving C, N, and /or H atoms increases (effect not shown in the figure). Besides, it must be pointed out the very low intensity of the emission peaks corresponding to atomic $H^*$ (i.e., $H_\alpha$, $H_\beta$, $H_\gamma$) and $O^*$ and that of the bands of $CH^*$ (A 4300 system) in most of the OES spectra registered for the $N_2$ mixtures, especially if compared with the previous experiments carried out in Ar.[15]

## IV. Discussion

A first evidence from the previous results is that NO can be effectively removed in a microwave SW cold plasma from a gas mixture with a composition very similar to that of real combustion streams. The fact that, even in the presence of oxygen, the use of $N_2$ as the carrier gas does not impede the decomposition of NO opens interesting questions regarding the plasma decomposition mechanisms. The explanation of the removal of NO and the induction of other secondary reactions depending on the gas mixtures requires a careful assessment of the possible reaction pathways for each particular gas composition. In the following we will discuss the possible reaction processes occurring for the different mixtures in relation with previously published data for plasma reactions with more simple gas mixtures.[5,6,13,21,24,29,30,34−36]

**A. Mixtures $N_2/NO$ and $N_2/NO/O_2$.** NO is efficiently converted into $N_2$ and $O_2$ when nitrogen is used as carrier gas. According to the known reactions taking place in nitrogen plasmas, ground-state $N(^4S)$ species formed by plasma decomposition of nitrogen[4,27,36] can effectively lead to the decomposition of the small amounts of NO existing in our gas mixture. Another alternative would be the involvement of $N(^2D)$ excited atoms, although many authors consider that they are rapidly converted to NO in the presence of oxygen.[24,36] Therefore, the most likely reaction process would be
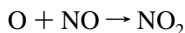
$$N(^4S) + NO(X) \rightarrow N_2(X,v) + O$$
$$k_1 = 3.0 \times 10^{-11} \text{ cm}^3/\text{s}, T = 298 \text{ K} \quad [37] \quad (1)$$
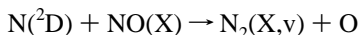
$$N(^2D) + NO(X) \rightarrow N_2(X,v) + O$$
$$k_2 = 4.5 \times 10^{-11} \text{ cm}^3/\text{s}, T = 298 \text{ K} \quad [37] \quad (2)$$

where NO(X) are ground-state molecules of this gas. The formation of atomic species of nitrogen in a SW plasma of nitrogen may proceed according to a large variety of processes as it is reported in Table 6. This table summarizes a series of plasma reactions taken from the literature and can be of importance to account for the results found in our experiments. Reactions T1 and T2, where electron impact processes are involved, can be an effective source of $N(^4S)$ and $N(^2D)$ atomic species and also of molecular metastable $N_2(A^3\Sigma_u^+)$ states. These species may transfer their energy to other species present in the discharge[24,27] (e.g., see reaction T4).

$N_2O$ in the range of traces has been detected as byproduct of the plasma reaction (cf., Table 1). Its formation very likely involves O atoms, as those produced through reaction 1 or reaction T4, this latter involving $N_2(A)$ excited molecules. These atomic oxygen species may then react according to
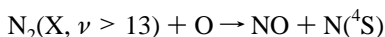
$$O + NO \rightarrow NO_2$$
$$k_3 = 3.0 \times 10^{-11} \text{ cm}^3/\text{s}, T = 200-1500 \text{ K} \quad [34] \quad (3)$$
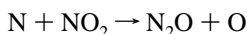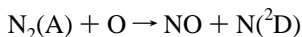
$$N + NO_2 \rightarrow N_2O + O$$
$$k_4 = 3.0 \times 10^{-12} \text{ cm}^3/\text{s}, T = 298 \text{ K} \quad [38] \quad (4)$$
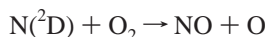
with $N_2O$ as a final reaction product.

In the presence of oxygen, the decomposition yield of NO decreases. This result is a consequence of the fact that oxygen produces a decrease in the electron temperature, thus making reactions less effective (eqs T1, T2). In addition, the production of some NO in parallel to its decomposition is another expected effect of the presence of oxygen in the plasma gas. These two effects are consistent with the small dissociation energy of $O_2$ as compared to that of $N_2$ and with the expected increase in the concentration of atomic oxygen as the $O_2$ in the mixture increases. In fact, atomic oxygen (O), either in the $O(^3P)$ or $O(^1D)$ states, can be effectively produced through reaction T3. Under these conditions, NO can be produced by collision of O or N atoms with $N_2$ and $O_2$ molecules as shown in reactions 5−8:

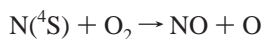$$N_2(X, v > 13) + O \rightarrow NO + N(^4S)$$
$$k_5 = 1.0 \times 10^{-13} \text{ cm}^3/\text{s}, T = 298 \text{ K} \quad [24] \quad (5)$$

$$N_2(A) + O \rightarrow NO + N(^2D)$$
$$k_6 = 7.0 \times 10^{-12} \text{ cm}^3/\text{s}, T = 298 \text{ K} \quad [36] \quad (6)$$

**1062** *J. Phys. Chem. A, Vol. 111, No. 6, 2007*

Hueso et al.

$$N(^2D) + O_2 \rightarrow NO + O$$
$$k_7 = 4.5 \times 10^{-11} \text{ cm}^3/\text{s}, \, T = 298 \text{ K} \ ^{39} \quad (7)$$

$$N(^4S) + O_2 \rightarrow NO + O$$
$$k_8 = 3.6 \times 10^{-15} \text{ cm}^3/\text{s}, \, T = 280-910 \text{ K} \ ^{40} \quad (8)$$

Reaction 5 may occur in discharges where $N_2$ molecules present a vibrational distribution characterized by the population of vibrational quantum numbers greater than 12.[23,24] Reaction 6 requires metastable states of the $N_2$ molecule which may also participate in the NO excitation processes (e.g., reaction T4). On the other hand, reactions 7 and 8 can be rather effective in producing NO if the amount of atomic nitrogen is high.[41] The activity of N atoms in producing NO was confirmed in previous experiments of our group where significant amounts of NO were produced in a SW plasma with Ar as carrier gas and $N_2$ and $O_2$ in small concentrations.[15]

Therefore, through reactions T3 and/or 4−8, the participation of oxygen will be a critical factor contributing to the decrease in the overall yield of NO decomposition in mixtures $N_2$/NO/$O_2$. An additional reaction pathway leading to the formation of NO is a wall process involving single N and O atoms at the wall of the discharge tube (i.e., N + O (wall) → NO (wall)).[42]

The previous plasma reaction scheme is supported by OES observations. Thus, for the mixture $N_2$/NO, we have detected the NO$\gamma$ system bands (230−290 nm) emitted by the excited state NO(A) (i.e., corresponding to the NO(A) → NO(X) + $h\nu$ deexcitation), this latter very likely produced through reaction T4. By contrast, the NO$\beta$ system bands (250−320 nm), emitted by NO(B) excited molecules,[25] are not detected in our system. This indicates that the concentration of NO(B) excited molecules, formed through a three-body reaction involving the combination of N($^4$S) and O atoms in the presence of $N_2$ or $O_2$, is negligible in our system.[24] The other spectral bands recorded under these conditions are the nitrogen first positive system (i.e., corresponding to the transition $N_2(B^3) \rightarrow N_2(A^3) + h\nu$) and the nitrogen second positive system (i.e., $N_2(C^3) \rightarrow N_2(B^3) + h\nu$). Note that $N_2(A^3)$ and $N_2(B^3)$ species are involved in reaction T5, which is very effective at pressures of the order of that used in our experiment.

In mixtures $N_2$/NO/$O_2$, the increase of the intensity of NO* bands with the concentration of oxygen in the plasma (cf. Figures 1, 2, and 4) is also in agreement with the previous reaction scheme. This observation supports an enhancement of the concentration of NO(A) excited species, even though reactions such as T6−T8 might simultaneously contribute to quench these states by reaction with $N_2$, $O_2$, or NO.[24]

In summary, the increase of the concentration of oxygen favors the formation of NO, detected in the NO$\gamma$ system (see Figure 1). Despite of the expected active role of the atomic N and O species, its rapid recombination does not permit its identification by OES, if compared with other carrier gases or experimental setups.[13,15,18] Nevertheless, some authors propose a titration method by adding Ar−NO mixtures to determine the density of atomic species from molecular bands,[28,43−45] although these measurements have not been carried out in this work due to the lack of $N_2$ pure discharge experiments.

**B. $N_2$/NO/$CH_4$.** The use of hydrocarbons as reductant compounds to improve the removal efficiency of $NO_x$ has been extensively studied both theoretically and experimentally.[1,16,32,46−48] When $CH_4$ is added to the $N_2$/NO mixture, NO is very effectively removed and new intermediate species can be detected by OES (Figure 2 (left)). The most remarkable

intermediate corresponds to CN* radicals giving rise to the bands of the violet and red emission systems (Table 2). These bands become more intense as the $CH_4$ content in the mixture increases (Figure 2 (right)). Moreover, NH* intermediates can be also recognized when methane is added to the gas mixture (see Figure 2 (center)). According to previous works in the literature,[30] the addition of $CH_4$ must contribute to the decrease in the concentrations of $N_2$(B) and $N_2$(C) states, responsible for the emission of the first and second positive systems of $N_2$*, as well as for generation of N($^4$S) atoms. A similar behavior is also expected in our system. A possible reaction by which a low concentration of $CH_4$ in the mixture would produce a sharp decrease in the concentration of N atoms is their direct reaction with $CH_x$ radicals produced by electron collisions with $CH_4$:[24,41,49]

$$N + CH_x \rightarrow CN + xH \quad (9)$$

$$2CH_4 + N \rightarrow CH + CN + 3H_2 + H \quad (10)$$
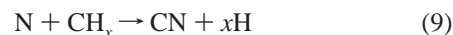
In comparison with our previous results using Ar as carrier gas,[15] reactions 9 and 10 can also explain the depletion of $C_2H_y$ and CH* excited species (A 4300 system) observed respectively by MS and OES. Additional reaction pathways for the formation of C atoms and subsequently CN species are proposed in reactions T9 and T10. In contrast to previous experiments in Ar,[15,50] there is a manifest absence of deposits of carbon and $C_2$* intermediate species when $N_2$ is used as the carrier gas. This fact is in part attributed to the presence of active N atoms in the nitrogen plasma and to the high activity of these species for the removal of carbon through its transformation into CN species.

The CN* radicals detected by OES must be the precursor species for the formation of the stable HCN, subsequently detected by MS (Table 3). Different routes are proposed by computational and experimental methods to account for the formation of this noxious product.[24,51] Some of the possible reactions involved are reported in Table 6 (reactions T11−T13).

Meanwhile, the simultaneous observation by OES and MS of NH* species in the plasma and $NH_3$ as a final product (cf., Tables 2 and 3) can be accounted for by a combination of reactions T13−T18 and T23. In turn, the formed NH* radicals can also participate actively in the formation and removal processes of NO, according to reactions T19−T22. The presence of N* and H* atomic lines (see Table 2) previously pointed out in the section IIIB might be indeed related to the direct dissociation and/or formation of NH*, since its intensities increase with the methane content (reaction T16). Concerning the atomic density of N, no quantitative data can be provided although we can assume qualitatively that the intensity of the band at 580.4 nm, used by Ricard et al.,[28,43−45] diminishes if compared with the $N_2$/NO/$O_2$ mixtures, which means that our system behaves in a way similar to that previously described in the literature.[28,43−45]

CO is another product detected by MS with the mixtures containing methane. The formation of this product should proceed by the reaction of O atoms dissociated from NO with other active species containing carbon such as CN and/or $CH_x$:

$$CN + O \rightarrow CO + N(^4S, \, ^2D)$$
$$k_{11} = 1.7 \times 10^{-11} \text{ cm}^3/\text{s}, \, T = 300-5000 \text{ K} \ ^{29} \quad (11)$$
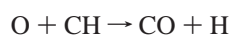
$$O + CH \rightarrow CO + H$$
$$k_{12} = 6.6 \times 10^{-11} \text{ cm}^3/\text{s}, \, T = 300-2500 \text{ K} \ ^{29} \quad (12)$$

**TABLE 5: Reaction Products for $N_2$ + NO + $CH_4$ + $O_2$ Mixtures Containing Different Concentrations of $CH_4$ and $O_2$**

| reacn mixture | NO removal (%) | $CH_4$ removal (%) | $O_2$ conversn (%) | reacn products (ppm) |
|---|---|---|---|---|
| $N_2$ + NO + $CH_4$ (0.3%) + $O_2$ (1%) | 90 | 97 | 42 | $H_2$, CO (<2300), $NH_3$, $H_2O$ (<8000), $CO_2$ (<500), $N_2O$ (traces) |
| $N_2$ + NO + $CH_4$ (0.3%) + $O_2$ (3%) | 67 | 97 | 14 | $H_2$, CO (<2000), $NH_3$, $H_2O$ (<6500), NO (<1000), $CO_2$ (<400), $N_2O$ (traces) |
| $N_2$ + NO + $CH_4$ (0.5%) + $O_2$ (1%) | 100 | 100 | 78 | $H_2$, CO (<3800), $NH_3$, $H_2O$ (<6500), $CO_2$ (<600), $N_2O$ (traces) |
| $N_2$ + NO + $CH_4$ (0.5%) + $O_2$ (3%) | 60 | 100 | 23 | $H_2$, CO (<3900), $NH_3$, $H_2O$ (<8400), $CO_2$ (<700), NO (<1200) |

**TABLE 6: Summary of Plasma Reactions Induced by MW Discharges That Can Be Involved in the Decomposition Processes Observed in This Work**

| no.[a] | reacns | rate constants $k_{298}$ (cm³ molecule⁻¹ s⁻¹) | temp range (K) | refs |
|---|---|---|---|---|
| T1 | e + $N_2$(X) → e + N($^4$S) + N($^4$S,$^2$D) | $f$ (E/N) | | 52 |
| T2 | e + $N_2$(X) → e + $N_2$(A) | $f$ (E/N) | | 40 |
| T3 | e + $O_2$ → e + O($^3$P) + O($^3$P,$^1$D) | $f$ (E/N) | | 53 |
| T4 | $N_2$(A) + NO(X) → $N_2$(X) + NO(A) | $6.4 \times 10^{-11}$ | | 54 |
| T5 | $N_2$(X,v) + $N_2$(A) → $N_2$(X) + $N_2$(B,v) | $2.0 \times 10^{-11}$ | | 54 |
| T6 | NO(A) + $N_2$ → NO(X) + $N_2$ | $1.0 \times 10^{-13}$ | | 24 |
| T7 | NO(A) + $O_2$ → NO(X) + $O_2$ | $1.5 \times 10^{-10}$ | | 24 |
| T8 | NO(A) + NO → NO(X) + NO | $1.0 \times 10^{-10}$ | | 24 |
| T9 | N + CN → C + $N_2$ | $6.6 \times 10^{-11}$ | | 42 |
| T10 | C + N + $N_2$ → CN(B,7) + $N_2$ | $1.5 \times 10^{-13}$ | | 42 |
| T11 | CN + $H_2$ → HCN + H | $1.5 \times 10^{-13}$ | | 30 |
| T12 | CN + $CH_4$ → HCN + $CH_3$ | $3.4 \times 10^{-10}$ | | 30 |
| T13 | N + $H_2$CN → HCN + NH | $6.7 \times 10^{-11}$ | | 30 |
| T14 | NO + H → HNO | $2.5 \times 10^{-10}$ | 300 | 55 |
| T15 | H + HNO → OH + NH | $2.4 \times 10^{-9}$ | 313 | 56 |
| T16 | $N_2$(A) + H → NH + N | $2.1 \times 10^{-10}$ | | 57 |
| T17 | N($^2$D) + $H_2O$ → NH + OH | $2.5 \times 10^{-10}$ | 200–300 | 39 |
| T18 | N($^2$D) + $H_2$ → NH(X) + H | $2.3 \times 10^{-12}$ | 200–300 | 58 |
| T19 | NH + NO → $N_2O$ + H | $5 \times 10^{-11}$ | 270–380 | 29 |
| T20 | NH + NO → $N_2$ + OH | $5 \times 10^{-11}$ | 270–380 | 29 |
| T21 | NH + OH → NO + $H_2$ | $8.0 \times 10^{-11}$ | 300–1000 | 29 |
| T22 | NH + O → NO + H | $6.6 \times 10^{-11}$ | | 29 |
| T23 | CN + OH → CO + NH | $1.4 \times 10^{-10}$ | 292 | 59 |
| T24 | CN + $O_2$ → CO + NO | $6.1 \times 10^{-12}$ | 292 | 59 |
| T25 | CN + $O_2$ → NCO + O | $2.2 \times 10^{-11}$ | 300–2500 | 29 |
| T26 | NCO + NO → $N_2O$ + CO | $3.3 \times 10^{-11}$ | 500–3000 | 29 |
| T27 | NCO + NO → $N_2$ + $CO_2$ | $3.3 \times 10^{-11}$ | 500–3000 | 29 |
| T28 | NCO + NO → $N_2$ + CO + O | $3.3 \times 10^{-11}$ | 500–3000 | 29 |
| T29 | H + CHO → $H_2$ + CO | $1.5 \times 10^{-10}$ | 300–2500 | 29 |
| T30 | $CO_2$ + CH → H + 2CO | $1.8 \times 10^{-12}$ | 300–1000 | 29 |
| T31 | $CO_2$ + $N_2$(A) → $N_2$ + CO + O | $7.2 \times 10^{-13}$ | | 39 |
| T32 | $CO_2$ + N($^2$D) → CO + NO | $1.3 \times 10^{-11}$ | | 39 |

[a] T1–T3: Electron impact dissociation processes. Coefficients are dependent on E/N values and electron energy distribution function (EEDF). T4: Only mechanism responsible for the NO(A) excited states production. T6–T8: Quenching processes of NO(A) species. T9–T13 and T23–T28: Kinetics involving CN* and HCN* species. T13–T23: Reactions for NH* intermediates. T23–T32: Processes related with CO* production. T31–T32: Reactions responsible for $CO_2$ back-reduction to CO.

Owing to the long average lifetime of CN* species,[30] the most likely reaction is one that involves these intermediates (i.e., reaction 11). In this way, CN* might also be a possible source of N($^4$S) excited states very active for the decomposition of NO (reaction 1).

In summary, the presence of increasing amounts of $CH_4$, beyond the further decomposition of NO, is favoring the formation of CN* and NH* intermediates, which might be also responsible of the raising presence of N and H atomic species, detected by OES, through reactions T11 and T16. Additionally, the formation of CO as product is determined by MS but not observed in the emission spectra and may occur through reactions 11 and 12 and T23 and T24.

**C. $N_2$/NO/$CH_4$/$O_2$.** A first glance to the results obtained with this mixture evidence that they are the convolution of those obtained for the $N_2$/NO/$CH_4$, $N_2$/$CH_4$/$O_2$, and $N_2$/NO/$O_2$ mixtures. Other evidence is that the concentration of the different minority components (i.e., $CH_4$ and $O_2$) is the key parameter for the control of the final removal efficiency of NO and the definition of the other byproducts formed in the reaction processes. Thus, when the relative concentrations of $O_2$ and $CH_4$

are 1% and 0.5%, practically 100% decomposition of NO is obtained. When the concentration of oxygen increases up to 3%, NO removal efficiency decreases down to 60%. From a practical point of view this might indicate that the solution for an effective NO removal would be to decrease the oxygen content in the mixture. However, this type of adjustments should be handled very carefully since HCN, a compound more noxious than NO, can then be formed in mixtures with little oxygen (cf. Table 4). It is also worth mentioning that in the present experiment, contrary to other plasma processes based on DBD discharges where $NO_2$ is formed,[5,6] only decomposition into $N_2$ and $O_2$ is found.

In mixtures $N_2$ (carrier) + NO + $CH_4$ + $O_2$, the actual $O_2$/ $CH_4$ ratio in the gas mixture is a critical parameter not only for the control of the final product composition but also for the determination of the intensity of the different bands monitored by OES. Thus, in comparison with the behavior observed for the $N_2$/NO/$CH_4$ mixture, the presence of $O_2$ seems to favor the oxidation of the intermediate species formed out of $CH_4$ (i.e., CN, CH, and NH) toward CO, $CO_2$, and $H_2O$ as final products (cf., Figure 4 (center and right)). Reactions T23–T32 are

proposed as possible additional processes occurring under our conditions to account for the evolution of reaction products reported in Table 5 and the evolution of the OES spectra in Figure 4. The atomic N and H species detected (see Table 2) respond in an way opposite to the increment of the oxygen percentage, since the intensity of the former decreases while the intensity of the latter increases. This fact again might be correlated with processes where NH intermediates intervene and reactions T16 and T22 are favored.

In conclusion, the experimental conditions described in the ternary mixtures are also reproduced in the quaternary ones. In these mixtures, oxygen is always present and that means that the intensity of CN, NH, and CH is reduced to minimum traces (Table 5), while the percentage of decomposition of NO is not so favored (see reactions 4−8). The same tendencies as in the ternary mixtures can be observed for the N and H atomic species, since the intensity of the former decreases and that of the latter increases, when the amount of oxygen is enhanced (reactions T16 and T22 in Table 6).

## V. Conclusions

The previous results and discussion have shown that NO can be efficiently removed by flowing plasmas from complex gas mixtures containing nitrogen as carrier gas and oxygen and hydrocarbons as minority components. The plasma processes involved in the reactions are very complex, and a precise control of the component gases is required if plasma abatement is to be used for practical NO removal. In fact, while increasing the oxygen concentration may prevent the formation of unwanted byproducts such as HCN or $NH_3$, a too high concentration of this gas (i.e., >3%) may drastically reduce the removal efficiency of NO. This implies that an effective use of flowing plasma processes for the removal of noxious gases requires a very strict control of the gas composition within very narrow margin of concentrations.

The observations made by OES and MS of respectively given intermediate species in the plasma and final reaction products have been rationalized by considering the information existing in the literature about elemental plasma reactions. However, a more detailed description of the reaction mechanisms involved with these complex plasma mixtures still requires more precise kinetic models accounting for all the meaningful parameters of the plasma discharge (i.e., actual temperature of species, effects of gases adsorbed in the walls, etc.).

## References and Notes

(1) Rajanikanth, B. S.; Srinivasan, A. D.; Ravi, V. *IEEE Trans. Dielectr. Electr. Insul.* **2005**, *12*, 72.

(2) Penetrante, B. M.; Hsiao, M. C.; Merritt, B. T.; Vogtlin, G. E.; Wallman, P. H.; Neiger, M.; Wolf, O.; Hammer, T.; Broer, S. *Appl. Phys. Lett.* **1996**, *68*, 3719.

(3) Chae, J. O. *J. Electrost.* **2003**, *57*, 251.

(4) Penetrante, B. M.; Brusasco, R. M.; Merritt, B. T.; Vogtlin, G. E. *Pure Appl. Chem.* **1999**, *71*, 1829.

(5) Penetrante, B. M.; Hsiao, M. C.; Merritt, B. T.; Vogtlin, G. E.; Wallman, P. H.; Kuthi, A.; Burkhart, C. P.; Bayless, J. R. *Appl. Phys. Lett.* **1995**, *67*, 3096.

(6) Dorai, R.; Kushner, M. J. *J. Phys. D: Appl. Phys.* **2001**, *34*, 574.

(7) Mok, Y. S.; Ham, S. W. *Chem. Eng. Sci.* **1998**, *53*, 1667.

(8) Rajanikanth, B. S.; Ravi, V. *Plasma Sci. Technol.* **2004**, *6*, 2411.

(9) Hu, X. D.; Zhang, J. J.; Mukhnahallipatna, S.; Hamann, J.; Biggs, M. J.; Agarwal, P. *Fuel* **2003**, *82*, 1675.

(10) Timmermans, E. A. H.; Jonkers, J.; Rodero, A.; Quintero, M. C.; Sola, A.; Gamero, A.; Schram, D. C.; van der Mullen, J. A. M. *Spectrochim. Acta, Part B* **1999**, *54*, 1085.

(11) Baeva, M.; Gier, H.; Pott, A.; Uhlenbusch, J.; Hoschele, J.; Steinwandel, J. *Plasma Chem. Plasma Process.* **2001**, *21*, 225.

(12) Al-Shamma's, A. I.; Wylie, S. R.; Lucas, J.; Pau, C. F. *J. Phys. D: Appl. Phys.* **2001**, *34*, 2734.

(13) Luo, J.; Suib, S. L.; Marquez, M.; Hayashi, Y.; Matsumoto, H. *J. Phys. Chem. A* **1998**, *102*, 7954.

(14) Castillo, M.; Herrero, V. J.; Tanarro, I. *Plasma Sources Sci. Technol.* **2002**, *11*, 368.

(15) Hueso, J. L.; González-Elipe, A. R.; Cotrino, J.; Caballero, A. *J. Phys. Chem. A* **2005**, *109*, 4930.

(16) Zhu, A. M.; Sun, Q.; Niu, J. H.; Xu, Y.; Song, Z. M. *Plasma Chem. Plasma Process.* **2005**, *25*, 371.

(17) Penetrante, B. M.; Hsiao, M. C.; Merritt, B. T.; Vogtlin, G. E.; Wallman, P. H. *IEEE Trans. Plasma Sci.* **1995**, *23*, 679.

(18) Luo, J.; Suib, S. L.; Hayashi, Y.; Matsumoto, H. *J. Phys. Chem. A* **1999**, *103*, 6151.

(19) Chae, J. O.; Hwang, J. W.; Jung, J. Y.; Han, J. H.; Hwang, H. J.; Kim, S.; Demidiouk, V. I. *Phys. Plasmas* **2001**, *8*, 1403.

(20) Rajanikanth, B. S.; Das, S.; Srinivasan, A. D. *Plasma Sci. Technol.* **2004**, *6*, 2475.

(21) Gentile, A. C.; Kushner, M. J. *J. Appl. Phys.* **1995**, *78*, 2074.

(22) Dorai, R.; Kushner, M. J. *J. Phys. D: Appl. Phys.* **2002**, *35*, 2954.

(23) Gordiets, B. F.; Ferreira, C. M.; Guerra, V. L.; Loureiro, J.; Nahorny, J.; Pagnon, D.; Touzeau, M.; Vialle, M. *IEEE Trans. Plasma Sci.* **1995**, *23*, 750.

(24) Pintassilgo, C. D.; Loureiro, J.; Guerra, V. *J. Phys. D: Appl. Phys.* **2005**, *38*, 417.

(25) Pointu, A. M.; Ricard, A.; Dodet, N.; Odic, E.; Larbre, J.; Ganciu, M. *J. Phys. D: Appl. Phys.* **2005**, *38*, 1905.

(26) Henriques, J.; Villeger, S.; Levaton, J.; Nagai, J.; Santana, S.; Amorim, J.; Ricard, A. *Surf. Coat. Technol.* **2005**, *200*, 814.

(27) Guerra, V.; Galiaskarov, E.; Loureiro, J. *Chem. Phys. Lett.* **2003**, *371*, 576.

(28) Diamy, A. M.; Hochard, L.; Legrand, J. C.; Ricard, A. *Surf. Coat. Technol.* **1998**, *98*, 1377.

(29) Baulch, D. L.; Cobos, C. J.; Cox, R. A.; Esser, C.; Frank, P.; Just, T.; Kerr, J. A.; Pilling, M. J.; Troe, J.; Walker, R. W.; Warnatz, J. *J. Phys. Chem. Ref. Data* **1992**, *21*, 411.

(30) Pintassilgo, C. D.; Loureiro, J.; Cernogora, G.; Touzeau, M. *Plasma Sources Sci. Technol.* **1999**, *8*, 463.

(31) Savinov, S. Y.; Lee, H.; Song, H. K.; Na, B. K. *Plasma Chem. Plasma Process.* **2003**, *23*, 159.

(32) Bromly, J. H.; Barnes, F. J.; Muris, S.; You, X.; Haynes, B. S. *Combust. Sci. Technol.* **1996**, *115*, 259.

(33) Pearse, R. W. B.; Gaydon, A. G. In *The Identification of Molecular Spectra*; Champan and Hall: New York, 1976.

(34) Atkinson, R.; Baulch, D. L.; Cox, R. A.; Hampson, R. F.; Kerr, J. A.; Troe, J. *J. Phys. Chem. Ref. Data* **1989**, *18*, 881.

(35) Atkinson, R.; Baulch, D. L.; Cox, R. A.; Hampson, R. F.; Kerr, J. A.; Rossi, M. J.; Troe, J. *J. Phys. Chem. Ref. Data* **1997**, *26*, 1329.

(36) Kossyi, I. A.; Kostinsky, A. Y.; Matveyev, A. A.; Silakov, V. P. *Plasma Sources Sci. Technol.* **1992**, *1*, 207.

(37) Herron, J. T.; Green, D. S. *Plasma Chem. Plasma Process.* **2001**, *21*, 459.

(38) Atkinson, R.; Baulch, D. L.; Cox, R. A.; Hampson, R. F.; Kerr, J. A.; Troe, J. *J. Phys. Chem. Ref. Data* **1992**, *21*, 1125.

(39) Herron, J. T. *J. Phys. Chem. Ref. Data* **1999**, *28*, 1453.

(40) Fernandez, A.; Goumri, A.; Fontijn, A. *J. Phys. Chem. A* **1998**, *102*, 168.

(41) Ricard, A.; Jaoul, C.; Gaboriau, F.; Gherardi, N.; Villeger, S. *Surf. Coat. Technol.* **2004**, *188−189*, 287.

(42) Pintassilgo, C. D.; Cernogora, G.; Loureiro, J. *Plasma Sources Sci. Technol.* **2001**, *10*, 147.

(43) Diamy, A. M.; Hochard, L.; Legrand, J. C.; Ricard, A. *Plasma Chem. Plasma Process.* **1998**, *18*, 447.

(44) Diamy, A. M.; Legrand, J. C.; Moritts, A.; Ricard, A. *Surf. Coat. Technol.* **1999**, *112*, 38.

(45) Jaoul, C.; Czerwiec, T.; Belmonte, T.; Ricard, A.; Michel, H. *Eur. Phys. J.: Appl. Phys* **2004**, *26*, 227.

(46) Orlandini, I.; Riedel, U. *J. Phys. D: Appl. Phys.* **2000**, *33*, 2467.

(47) Dorai, R.; Kushner, M. J. *J. Appl. Phys.* **2000**, *88*, 3739.

(48) Niessen, W.; Wolf, O.; Schruft, R.; Neiger, M. *J. Phys. D: Appl. Phys.* **1998**, *31*, 542.

(49) Pereira, J.; Massereau-Guilbaud, V.; Geraud-Grenier, I.; Plain, A. *Plasma Process. Polym.* **2005**, *2*, 633.

(50) Heintze, M.; Magureanu, M.; Kettlitz, M. *J. Appl. Phys.* **2002**, *92*, 7022.

(51) Andersson, S.; Markovic, N.; Nyman, G. *J. Phys. Chem. A* **2003**, *107*, 5439.

(52) Cosby, P. C. *J. Chem. Phys.* **1993**, *98*, 9544.

Removal of NO by Flowing Microwave Discharges

*J. Phys. Chem. A, Vol. 111, No. 6, 2007* **1065**

(53) Cosby, P. C. *J. Chem. Phys.* **1993**, *98*, 9560.

(54) Guerra, V.; Sa, P. A.; Loureiro, J. *J. Phys. D: Appl. Phys.* **2001**, *34*, 1745.

(55) Cohen, N.; Westberg, K. R. *J. Phys. Chem. Ref. Data* **1991**, *20*, 1211.

(56) Forte, E. N. *J. Photochem.* **1981**, *17*, 13.

(57) Ho, G. H.; Golde, M. F. *J. Chem. Phys.* **1991**, *95*, 8866.

(58) Dodd, J. A.; Lipson, S. J.; Flanagan, D. J.; Blumberg, W. A. M.; Person, J. C.; Green, B. D. *J. Chem. Phys.* **1991**, *94*, 4301.

(59) Decker, B. K.; Macdonald, R. G. *J. Phys. Chem. A* **2003**, *107*, 9137.